

Anti-HER2 functionalized graphene oxide as survivin-siRNA delivery carrier inhibits breast carcinoma growth in vitro and in vivo

Xiaoli Wang¹⁻³Qi Sun¹⁻³Chunying Cui¹⁻³Jing Li¹⁻³Yifan Wang¹⁻³

¹Department of Pharmaceutics, School of Pharmaceutical Sciences, Capital Medical University, Beijing, China; ²Beijing Area Major Laboratory of Peptide and Small Molecular Drugs, Capital Medical University, Beijing, China; ³Engineering Research Center of Endogenous Prophylactic of Ministry of Education of China, Capital Medical University, Beijing, China

Background: The success of gene therapy is mostly dependent on the development of gene carrier. Graphene oxide (GO) possesses excellent aqueous solubility and biocompatibility, which is important for its biochemical and medical applications. Our previous work proved that GO can deliver siRNA into cells efficiently and downregulate the expression of desired protein.

Methods: In this study, a novel delivery carrier, GO-R8/anti-HER2 (GRH), was developed by conjugating octaarginine (R8) and anti-HER2 antibody with GO as a tumor active-targeting vector for survivin-siRNA delivery.

Results: GRH/survivin-siRNA formed nanoglobes of 195 ± 10 nm in diameter. Real-time polymerase chain reaction analysis revealed that survivin messenger RNA expression showed a $42.4\% \pm 2.69\%$ knockdown. The expression of survivin protein was downregulated to $50.86\% \pm 2.94\%$ in enzyme-linked immunosorbent assay. In MTT tests, GRH exhibited no testable cytotoxicity. In vivo, GRH/survivin-siRNA showed gene silencing and inhibition of tumor growth.

Conclusion: The in vitro and in vivo results consistently demonstrated that GRH/survivin-siRNA has potential to be an efficient gene silencing carrier for siRNA delivery in cancer therapy.

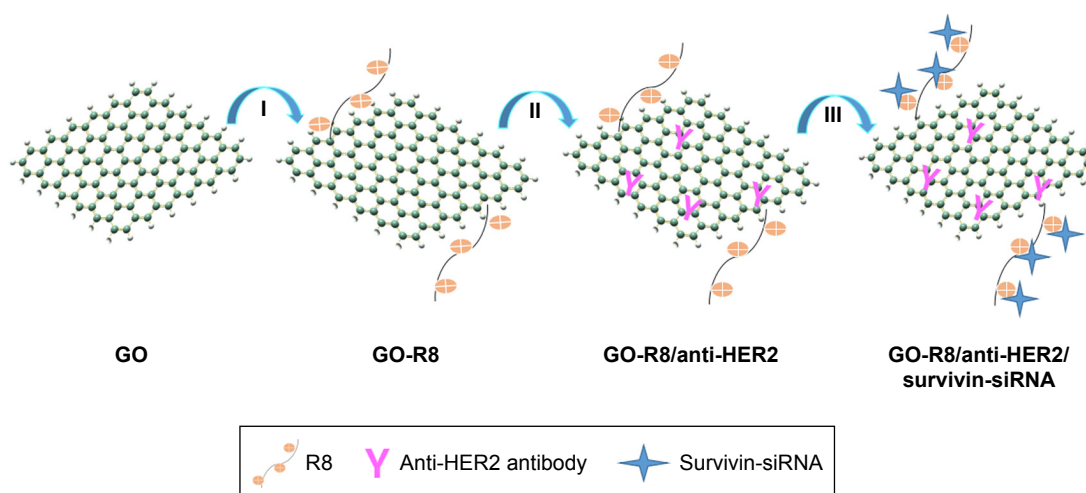
Keywords: graphene oxide, GO, survivin-siRNA, anti-HER2 antibody, small interfering RNA, gene delivery, nanocarrier

Introduction

RNA interference (RNAi) technique is an effective method to suppress protein expression by targeted cleavage of mRNA.¹ siRNA is a 21–23 nucleotide double-stranded RNA molecule, which participates in the RNA-induced silencing complex and induces the degradation of target mRNA.² Recently, clinically siRNA has been considered as a significant antitumor strategy. It is difficult to deliver the naked siRNA to the cells because of its large molecular weight and negative charge. Additionally, naked siRNA is easily susceptible to enzymatic degradation in vivo.^{3,4} Efficient and specific delivery of siRNA to cells or tissues has become one of the challenges of RNAi technology.

Graphene is a new kind of carbon nanostructure material, which has attracted much attention in the past decade.⁵⁻⁸ Previous research had shown that graphene oxide (GO) can be used as a delivery vector for anticancer drug, protein, and gene.⁶⁻¹³ The application of GO as a delivery carrier to deliver oligonucleotides for gene therapy has been reported in a few studies.^{12,14,15} In recent years, GO as a carrier for siRNA has shown broad prospects. For instance, Wang et al¹⁶ developed a GO-based gene delivery system by covalently conjugating polyethylene glycol (PEG) and polyethylenimine (PEI) to GO nanosheet

Correspondence: Chunying Cui
Department of Pharmaceutics, School of Pharmaceutical Sciences, Capital Medical University, 10 Youanmenwai Street, Fengtai, Beijing 100069, People's Republic of China
Tel +86 10 8391 1668
Email ccy@ccmu.edu.cn



Scheme 1 Synthetic route to preparing GO-R8 and GO-R8/anti-HER2/survivin-siRNA.

Notes: I: MES buffer, NHS, and EDAC, at room temperature. II: DI water, at room temperature. III: incubation at room temperature for 30 minutes.

Abbreviations: GO, graphene oxide; R8, octaarginine; GRH, GO-R8/anti-HER2; DI, deionized; MES, 2-morpholinoethanesulfonic acid; NHS, N-Hydroxysuccinimide; EDAC, 1-Ethyl-3-(3-dimethylaminopropyl) carbodiimide.

to improve its stability and gene transfection efficiency and reduce its cytotoxicity in serum conditions. With such superior phototherapy-enhanced gene delivery ability, the fabricated NGO-PEG-PEI has demonstrated to be a promising candidate for combined gene and photothermal therapies. Feng et al¹⁷ prepared PEI-PEG-functionalized GO to deliver pDNA and siRNA to enhance the delivery efficiency. The PEG conjugation along with π - π stacked pyrenemethylamine had been performed for the functionalization of GO to deliver siRNA into cancer cells.¹⁸ Cell-penetrating peptides (CPPs), such as octaarginine (R8), was used to modify GO and enhance the effect of siRNA delivery.¹⁹ GO-R8 was further labeled with anti-HER2 to bind with HER2, a transmembrane tyrosine kinase receptor overexpressed in 25%–30% of human breast cancer.²⁰ Survivin is the most recently identified, structurally unique member of the inhibitor of apoptosis protein family. Survivin protein is an inhibitor of apoptosis, whose overexpression is often observed in tumor cells.^{21,22} Survivin mediates its effects by strengthening the survival of tumor cells primarily through its antiapoptotic function.²³ It is specifically expressed in carcinomas and developing cells, which undergo either inappropriate or programmed cell growth by binding to mitotic spindle fibers. In addition, it causes cells to enter the S phase of the cell cycle and controls apoptosis by inhibiting apoptosis pathways.²⁴ The inhibition of survivin is considered to be an effective way to promote tumor cells apoptosis and lead to the death of tumor cells.

In this study, a novel R8 and anti-HER2 antibody (anti-HER2)-functionalized GO, as a gene carrier system, was strategically designed and prepared. Through the modification

of GO by octaarginine (R8) and anti-HER2 antibody, preparation of a schematic diagram, as shown in Scheme 1. The final carrier has the ability to specifically recognize the tumor cells on the transfect cells. The effective transfer and the expression of related gene both in vitro and in vivo were studied in the breast carcinoma cell line MCF-7.

Materials and methods

Materials

GO sheet was obtained from Sigma-Aldrich Co. (St Louis, MO, USA). Octaarginine (R8) was purchased from GL Biochem Ltd (Shanghai, China). Anti-HER2 antibody was obtained from Abcam (Cambridge, UK). Dialysis membranes (molecular weight cut off: 8 kD and 14 kD) were purchased from Spectrum labs (Los Angeles, CA, USA). The MCF-7 breast cancer cell line was obtained from Chinese academy of medical science tumor cells bank. Fetal bovine serum (FBS), RPMI-1640 medium, HyQ trypsin, and PBS were obtained from Hyclone (Logan, UT, USA). Hoechst 33342 was purchased from Thermo Fisher Scientific (Waltham, MA, USA). Survivin-siRNA, carboxyfluorescein (FAM)-survivin-siRNA, and negative control (NC) siRNA were all purchased from GL Biochem Ltd. Lipo™ 2000 was purchased from Thermo Fisher Scientific. Penicillin and streptomycin were purchased from Sigma Chemicals (Perth, Australia). RPMI-1640 medium, FBS, and trypsin were provided by Hyclone. DMSO was purchased from AppliChem GmbH Company (Darmstadt, Germany). BCA protein kit was purchased from Pierce (Rockford, IL, USA). Human survivin ELISA kit and mouse survivin

ELISA kit were purchased from Thermo Fisher Scientific. High-capacity cDNA reverse transcription kit, high-capacity RNA-to-cDNA Kit, TaqMan gene expression master mix, and TaqMan Gene Expression Assays (survivin assay, GAPDH assay) were obtained from Thermo Fisher Scientific. Trizol was obtained from Thermo Fisher Scientific. Other chemicals and reagents were of chemical grade unless otherwise specified. The sequences of mus-survivin-siRNA are 5'-CCGAGAACGAGCCUGAAUUTT-3' (sense) and 5'-AAAUCAGGCUCGUUCUCGGTT-3' (antisense). The sequences of homo-survivin-siRNA are 5'-CACCGCAUCUCUCUACAUCATT-3' (sense) and 5'-UGAAUGUAGAGAGAUGC GGUGTT-3' (antisense). The sequences of NC are 5'-UUCUCCGAACGUGUCACGUTT-3' (sense) and 5'-ACGUGACA CGUUCGGAGAATT-3' (antisense).

Instruments

Infrared spectrometer (Nicolet iS5; Thermo Fisher Scientific), UV-vis spectrophotometer (UV-2600, Shimadzu, Kyoto, Japan), zeta potential instrument ZetaPlus (Brookhaven Instruments Corporation, NY, USA), differential scanning calorimeter (DSC, 204F1; Netzsch, Germany), transmission electron microscope (TEM; JEOL, Tokyo, Japan), UV transilluminator (Geliance 600, PerkinElmer Inc., Waltham, MA, USA), microplate reader (SpectraMax M3; Molecular Devices LLC, Sunnyvale, CA, USA), confocal laser scanning microscope (Leica Microsystems, Wetzlar, Germany), nanodrop spectrophotometer (Nano-1000; Thermo Fisher Scientific), real-time PCR System (7500, Thermo Fisher Scientific), and inverted microscope (IX71, Olympus Corporation, Tokyo, Japan) were used.

Preparation of GO-R8/anti-HER2 (GRH)/survivin-siRNA

Preparation of nanographene oxide sheets (NGOS)

GO sheets (1 mg) were dispersed in 1 mL deionized (DI) water under sonication for 30 minutes, and chloroacetic acid solution in 4 M NaOH was prepared. The latter suspension was immediately added into the former mixture under the condition of ice bath. The suspension was reacted for 4 hours ultrasonically and then stirred at room temperature for another 1 hour. The solution was centrifuged, washed with H₂O for 3 times at 12,000 × *g* for 20 minutes, collected, and freeze-dried.²⁵

Preparation of GO-R8

GO-R8 was prepared through previous method.²⁶ It was performed through 2-step method. In brief, 5 mg of NGOS was

first added to the 5 mL DI water and sonicated for 1 hour. After that, 2.5 mL of 500 mM 2-morpholinoethanesulfonic acid (MES) buffer solution (pH 6.1) and 2.5 mL of a 50 mg/mL N-hydroxysuccinimide solution were added into the suspension and stirred for 15 minutes. Then, 3 mL of 1-Ethyl-3-(3-dimethylaminopropyl) carbodiimide solution (10 mg/mL) was added to the former suspension and stirred for 0.5 hour at room temperature, and the mixture was centrifuged and suspended with 50 mM MES buffer solution (pH 6.1). Subsequently, 15 mg of R8 in 15 mL MES buffer was added to the mixture and stirred for 24 hours at room temperature. After that, the obtained GO-R8 was centrifuged and washed with MES buffer for 3 times.

Preparation of GRH

10 μL of anti-HER2 (1 mg/mL) was added to the 4 mL of GO-R8 (0.7 mg/mL) solution and stirred at room temperature for 24 hours.²⁷ After that, the product was separated from solution, washed with DI water, centrifuged at 12,000×*g* for 15 minutes, and then washed with PBS for 3 times.

Preparation of GRH/survivin-siRNA

Survivin-siRNA (1 μg) was mixed with different mass ratios of nanoparticle samples (N/P=10:1, 15:1, 20:1, 25:1, 30:1, 35:1, and 40:1). The complexes were incubated at room temperature for 0.5 hour.^{28–30}

Characterization

The morphology was examined by TEM. Zeta potential, hydrodynamic size, and optical property were measured using a zeta potential analyzer. The structures of GO, R8, GO-R8, and GRH were characterized by Fourier-transform infrared spectroscopy (FTIR) spectra and UV-vis absorption spectra. UV-vis absorption was measured using an UV-vis spectrophotometer (water served as a solvent).

Degradation of GRH/survivin-siRNA heparin and anti-RNase A

Heparin is a kind of mucopolysaccharide, with many anionic groups on the polysaccharide chain, such as sulfonic acid group, carboxyl group, etc. Therefore, heparin is highly electronegative and can be combined with the cationic group. Because of negative charge, siRNA can be replaced by heparin from the functional GO-R8/HER2. With a strong negative charge, heparin can combine with siRNA to form a new complex. Therefore, the survivin-siRNA loaded onto GRH can be replaced by heparin. In this experiment, the

naked survivin (NS)-siRNA and RNaseA are coincubated for 0 minute, 5 minutes, 15 minutes, 30 minutes, 45 minutes, and 60 minutes, and then GRH/survivin-siRNA and RNaseA are coincubated for another 0 hour, 0.5 hour, 1 hour, 1.5 hours, 6 hours. The samples were added into the agarose gel, respectively, and the complexes were carried out in TE buffer at a constant voltage of 120 V for 20 minutes.³¹ The result was recorded using an UV transilluminator.

Agarose gel retardation assay

Gel electrophoresis was used to evaluate the ability of siRNA loading and complexation of GRH.⁴ According to the method mentioned in the "Preparation of GRH/survivin-siRNA" section, the samples were added into the agarose gel, respectively, and the complexes were carried out in TE buffer at a constant voltage of 120 V for 20 minutes. The result was recorded using an UV transilluminator.

Calorimetric analysis

DSC was used for evaluating the absorption of survivin-siRNA onto GRH.³² GO (10.56 μL , 1 $\mu\text{g}/\mu\text{L}$), GRH (10.56 μL , 1 $\mu\text{g}/\mu\text{L}$), and GRH/survivin-siRNA (10.56 μL , concentration of survivin-siRNA: 20 nM, 40 nM, 120 nM, and 160 nM) were heated, respectively, in a pierced aluminum pan from 20°C–200°C (scan at 20°C/min), and the DSC curves were recorded. Finally, the samples were cooled to 20°C at a rate of –40°C/min.

Cell culture

MCF-7 cells were cultured in 1640 medium containing 10% FBS, streptomycin (100 $\mu\text{g}/\text{mL}$), and penicillin (100 $\mu\text{g}/\text{mL}$) in humidified atmosphere containing 5% CO_2 at 37°C. MCF-7 cells were cultured to 70%–80% confluence for use.

Confocal image of GRH/survivin-siRNA-treated MCF-7 cells

Intracellular location of GRH/survivin-siRNA was investigated by confocal lasers scanning microscopy (LEICA TCS SP5; Leica Microsystems). Human breast cancer MCF-7 cells were cultured with the density of 3×10^5 per confocal dish (diameter, 20 mm) and incubated overnight at 37°C under 5% CO_2 24 hours. Before transfection, the cells were rinsed with PBS solution and cultured in 1640 medium without 10% FBS. Then, the cells were treated with 100 nM of survivin-siRNA, GRH/survivin-siRNA, Lipo 2000/survivin-siRNA, and culture medium. Culture medium was used as a blank control; NS-siRNA was used as a NC, whereas Lipo

2000/survivin-siRNA was used as a positive control. The 4 groups were incubated for another 4 hours, the medium of per confocal dish was discarded, and rinsed for 3 times with PBS. The cells were incubated with culture medium containing 1 $\mu\text{g}/\text{mL}$ of Hoechst 33342 for 15 minutes at room temperature. After washing the cells with PBS for 3 times, the cells were excited at 492 nm and emitted at 518 nm. The images were analyzed using Leica CLSM software.

Antiproliferation assay

The viability and proliferation of cells were evaluated using MTT assay in triplicate. MCF-7 cells (5×10^5 cell/well) were seeded into 96-well plates and were incubated for 24 hours. The cells were transfected with GRH, survivin-siRNA, GRH/NC, GRH/survivin-siRNA, Lipo 2000/NC, and Lipo 2000/survivin-siRNA at the concentration of 30 nM, 60 nM, 90 nM, 120 nM, and 150 nM for 48 hours. 25 μL of sterile MTT solution (5 mg/mL) was added into each well, and the cells were cultured at 37°C for 4 hours, and then the medium in 96-well plates was removed. 200 μL of DMSO was added into each well, and the 96-well plates were shaken for 15 minutes. The OD was measured at 570 nm. All experiments were repeated for 3 times.

Real-time polymerase chain reaction (PCR)

Real-time PCR is a powerful tool to quantify gene expression.^{33,34} In this study, real-time PCR was used to evaluate the expression of survivin-mRNA. MCF-7 cells were seeded into 6-well dishes at a density of 2×10^5 cell/well and were transfected by 100 nM of survivin-siRNA, GRH/NC, GRH/survivin-siRNA, Lipo 2000/NC, and Lipo 2000/survivin-siRNA for 48 hours. Trizol reagent was added to extract the total RNA on ice. Nanodrop-1000 was used to measure the concentration of the RNA content. 2 μg of RNA was reverse transcribed into cDNA by PCR amplification instrument, and the concentration of cDNA was measured. Primer pairs for survivin were synthesized and purified by GenePharma Co., Ltd. (Shanghai, China). The mRNA expression of survivin was evaluated against GAPDH mRNA. The Ct value was calculated using delta-delta Ct ($2^{-\Delta\Delta\text{Ct}}$) method. All experiments were repeated for 3 times.

ELISA

MCF-7 cells were seeded into 6-well plates at a density of 2.0×10^5 cells per well. The cells were transfected with 100 nM of survivin-siRNA, GRH/NC, GRH/survivin-siRNA, Lipo 2000/NC, and Lipo 2000/survivin-siRNA for 48 hours. Cells treated with PBS solution served as

blank, and Lipo 2000/survivin-siRNA was used as a positive control. The whole cell protein was extracted, and all operations were carried out on ice. The transfected cells were harvested and lysed with RIPA lysis buffer (NaCl [150 mM], NP-40 [1%], deoxycholate [0.5%], SDS [0.1%], Tris-HCl [50 mM, pH 7.5], and protease inhibitor cocktail [1%]). The concentration of protein was measured using a BCA Protein Assay kit. Lysates of protein (30 μ g) were prepared, and the amount of secreted survivin-siRNA was measured using a survivin ELISA kit (Thermo Fisher Scientific) according to the kit instructions. All experiments were repeated for 3 times.

In vivo antitumor assay

Male Institute of Cancer Research (ICR) mice (6-week-old, 18–32 g) were purchased from animal department of Capital Medical University (Beijing Laboratory Animal Center, Beijing, China) and raised at room temperature ($23^{\circ}\text{C}\pm 2^{\circ}\text{C}$). All care and handling of animals were approved by Institutional Authority for Laboratory Animal Care of Capital Medical University. All animal work was performed in accordance with the Health Guidelines of the Capital Medical University, and the Institutional Animal Ethics Committee of Capital Medical University approved the protocols. Tumor xenograft was made by inoculating S180 cells (200 μ L, 1.0×10^7 cells/mL) into the right armpits of ICR mice (6-week-old, male, 18–32 g). Tumor volumes were measured with a dial caliper and calculated according to the formula: volume (mm^3) = length \times width²/2. After a week, all mice were randomly divided into 4 groups ($n=10$). Four groups of mice were treated with GRH/survivin-siRNA (survivin-siRNA: 0.3 mg/kg and 12 mg/kg), NS-siRNA (0.3 mg/kg), doxorubicin (2 μ mol/kg), and saline (0.2 mL/mice). The mice were intravenously injected with 0.2 mL volume at every other day for a total of 5 times. After 10 days, the mice were executed to harvest the heart, liver, spleen, lung, kidney, brain, and tumor. The tumor weight and body weight were measured, and the inhibiting tumor rate was calculated.

Tumor-targeting efficiency of GRH/survivin-siRNA in vivo

Tumor xenograft of each mice was made by inoculating 2×10^6 tumor cells into the right armpits of ICR mice (6-week-old, male, 18–32 g). The cancer-bearing mice were then divided into 4 groups randomly ($n=10$). Four groups of mice were treated with GRH/survivin-siRNA (survivin-siRNA: 0.3 and 12 mg/kg), GO-R8/survivin-siRNA (survivin-siRNA: 0.3 and 12 mg/kg), doxorubicin (2 μ mol/kg), and saline

(0.2 mL/mice). The mice were intravenously injected with 0.2 mL volume at every other day for a total of 5 times. After 10 days, the mice were executed to harvest the tumor. The tumor weight was measured.

Cytotoxicity

The cytotoxicity of GRH against MCF-7 cells was evaluated using MTT assay in triplicate. MCF-7 cells were seeded into 96-well plate at a density of 4×10^3 per well in 100 μ L of medium and cultured overnight. The wells were incubated in medium containing 5–120 μ g/mL of GRH in 25 μ L medium for 48 hours. The following experimental steps were same with the method in the “Antiproliferation assay” section. Finally, the absorbance was measured at 490 nm. All experiments were repeated for 3 times.

Results and discussion

FTIR, UV-vis, TEM, zeta potential, and Tyndall effect

FTIR measurement was used to confirm the successful preparation of GRH. Spectra of GO, R8, GO-R8, and GRH are shown in Figure 1. FTIR spectra show a broad peak of CO_2H groups at $3,200\text{--}3,500\text{ cm}^{-1}$. Compared with the FTIR spectrum of GO, the spectrum of GO-R8 showed a broad peak of CO_2H groups at $3,200\text{--}3,500\text{ cm}^{-1}$ (broad absorption peak of O–H stretching vibration), the peak of the carbonyl groups of the amide at $\sim 1,680\text{ cm}^{-1}$, suggesting that R8 was covalently coupled with the GO successfully. The peak at $1,640\text{ cm}^{-1}$ in the spectrum of GRH indicated the presence of C=O stretching vibration, which is the evidence of combination of GO-R8. The strong absorption peaks of amide I ($1,640\text{ cm}^{-1}$) and amide II ($1,510\text{ cm}^{-1}$) were caused by amidation between GO-R8 and GRH.

Figure 2 shows that the UV-vis spectra of R8, GO, and GO-COOH had characteristic absorption peaks at 207 nm (yellow), 230 nm (blue), and 234 nm (red), respectively. After GO-R8 formation, the absorption peaks appear at around 200–270 nm (green), which is attributed to the amidation and reduction of GO-COOH after the R8 peptide conjugation. These 2 characteristic peaks also exist in the anti-HER2-labeled GO-R8.

Figure 3 shows the visualized morphology of GO and GRH by TEM. It was found that GRH had the smaller diameter size from 90 to 210 nm in comparison with the smooth surface of GO sheets with the diameter size from 120 to 260 nm.

Figure 4 shows that the zeta potentials of GO, GO-R8, and GRH were $-49.05 \pm 3.81\text{ mV}$, $29.7 \pm 0.33\text{ mV}$, and

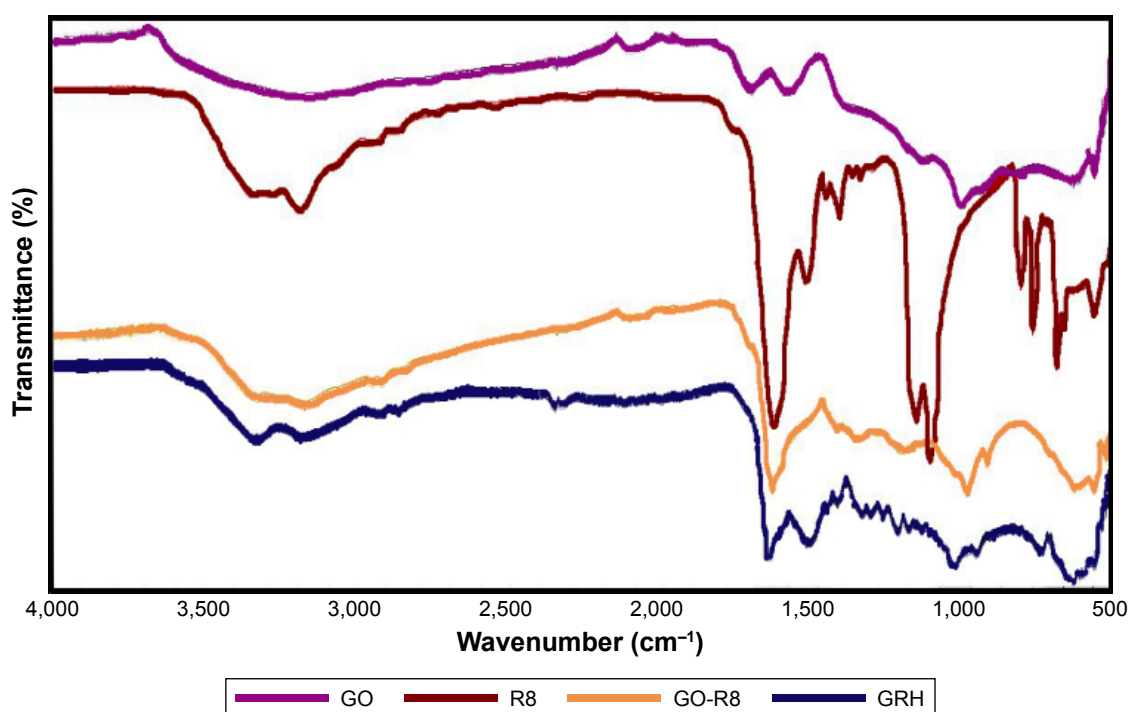


Figure 1 FTIR spectra of GO, R8, GO-R8, and GRH.

Abbreviations: FTIR, Fourier-transform infrared spectroscopy; GO, graphene oxide; GRH, GO-R8/anti-HER2; R8, octaarginine.

26.27±0.40 mV, respectively, which were beneficial to the cellular uptake. Figure 4C shows that the Tyndall phenomenon was observed clearly, which indicated that GO and GRH dispersed in nanosuspensions.³⁵

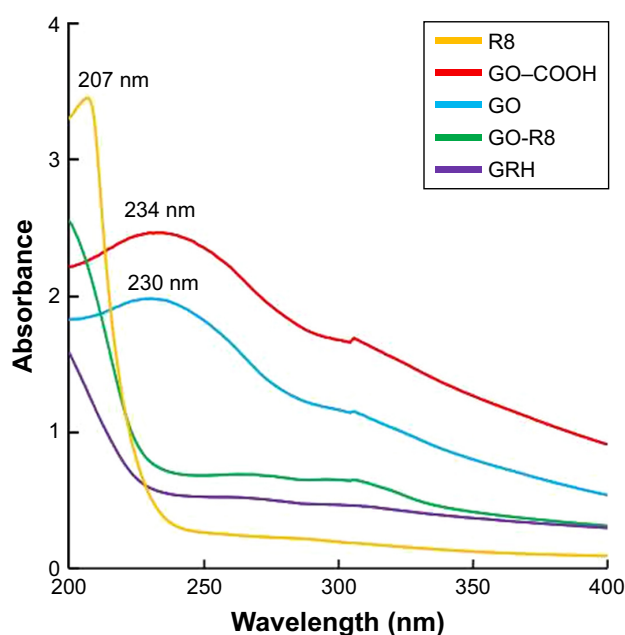


Figure 2 The UV-vis spectra of R8, GO-COOH, GO, GO-R8, and GRH.

Abbreviations: GO, graphene oxide; R8, octaarginine; GRH, GO-R8/anti-HER2.

Degradation of GRH/survivin-siRNA heparin and anti-RNaseA

Figure 5 shows that the NS-siRNA was completely degraded by RNaseA within 5 minutes. However, GRH/survivin-siRNA could protect siRNA from degrading with RNaseA until 6 hours. All of these results suggested that the GRH was a vector with well-protective effect for survivin-siRNA.

Gel retardation assay

The gel retardation assay was performed to confirm the electrostatic adsorption by survivin-siRNA and GRH. The retardation result of GRH and survivin-siRNA (w/w) is depicted in Figure 6. NS-siRNA was used as blank control, and the free siRNA was seen as bright band on the gel. When the ratio of GRH and survivin-siRNA reached 40:1 (w/w), the bright RNA band was totally invisible, which indicated that 1.0 mg of survivin-siRNA could be absorbed onto 40 mg of GRH effectively (Figure 6B). GRH/survivin-siRNA was prepared using the N/P ratio of 40:1 (w/w) at the following experiments. However, GO could not retard the migration of survivin-siRNA under the electrical field as shown in Figure 6A. Therefore, surface modification of GO was necessary for the survivin-siRNA loading.

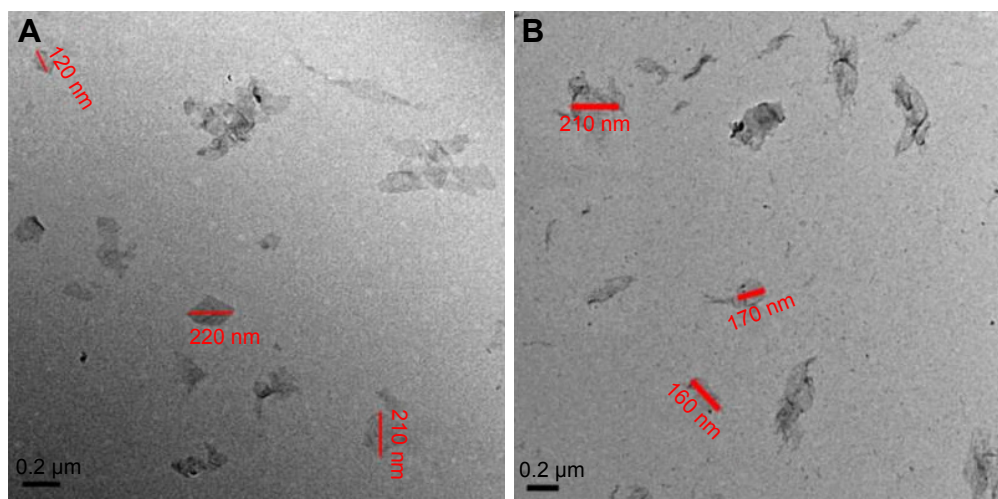


Figure 3 TEM images of GO (A) and GRH (B).

Abbreviations: TEM, transmission electron microscope; GO, graphene oxide; GRH, GO-R8/anti-HER2; R8, octaarginine.

DSC

The loading of survivin-siRNA onto GRH was analyzed with DSC, and shown in Figure 7. With the increase in the loading survivin-siRNA, the endothermic peaks shifted from 149.3°C to 157.3°C. With the increase in survivin-siRNA concentration, the peak value of the corresponding

concentration of DSC also increases, indicating the effective connection between the GRH and survivin-siRNA. The interactions between GRH and survivin-siRNA led to the changes in the DSC curves,^{36,37} which indicated that survivin-siRNA was effectively loaded onto GRH.

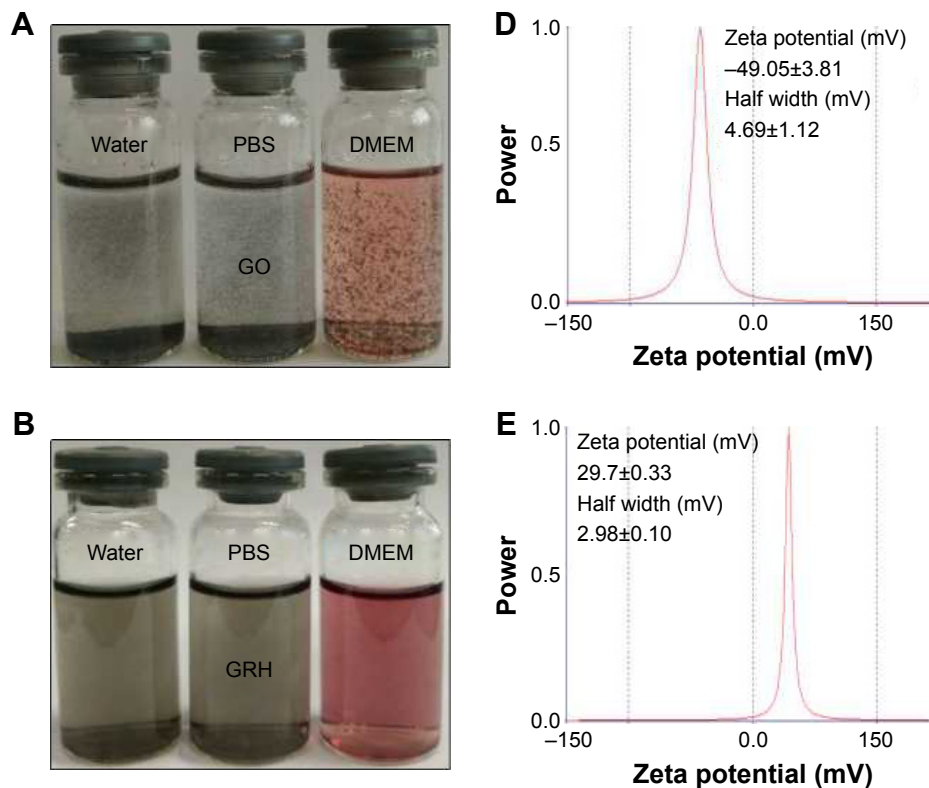


Figure 4 (Continued)

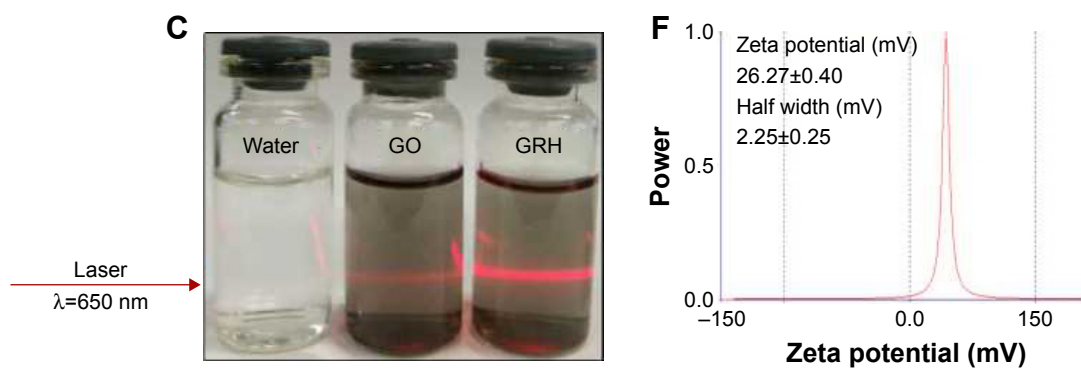


Figure 4 The dispersibility and stability of GO (A) and GRH (B), the Tyndall effect of GO and GRH (C), and the zeta potential of GO (D), GO-R8 (E), and GRH (F).
Abbreviations: GO, graphene oxide; GRH, GO-R8/anti-HER2; R8, octaarginine; DMEM, Dulbecco's Modified Eagle Medium; PBS, phosphate buffer saline.

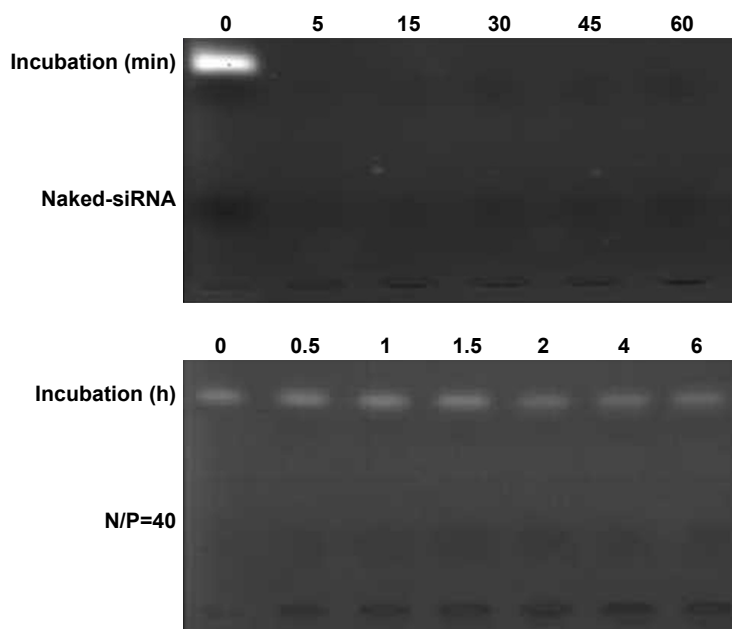


Figure 5 Degradation of GRH/survivin-siRNA heparin and anti-RNase A.

Note: N/P is the ratio of nitrogen to phosphorus.

Abbreviations: GRH, GO-R8/anti-HER2; GO, graphene oxide; R8, octaarginine; min, minutes; h, hours.

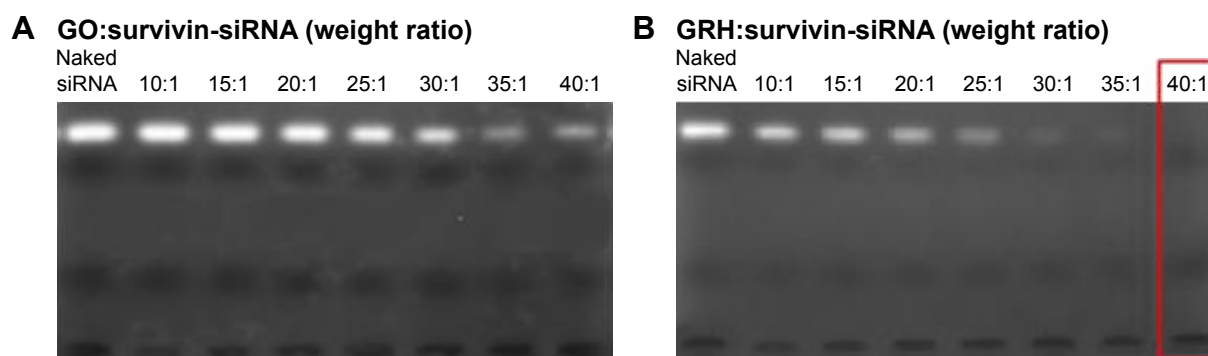


Figure 6 Agarose gel retardation assay of survivin-siRNA complexed with GO (A) and GRH (B).

Abbreviations: GO, graphene oxide; GRH, GO-R8/anti-HER2; R8, octaarginine; min, minutes; h, hours.

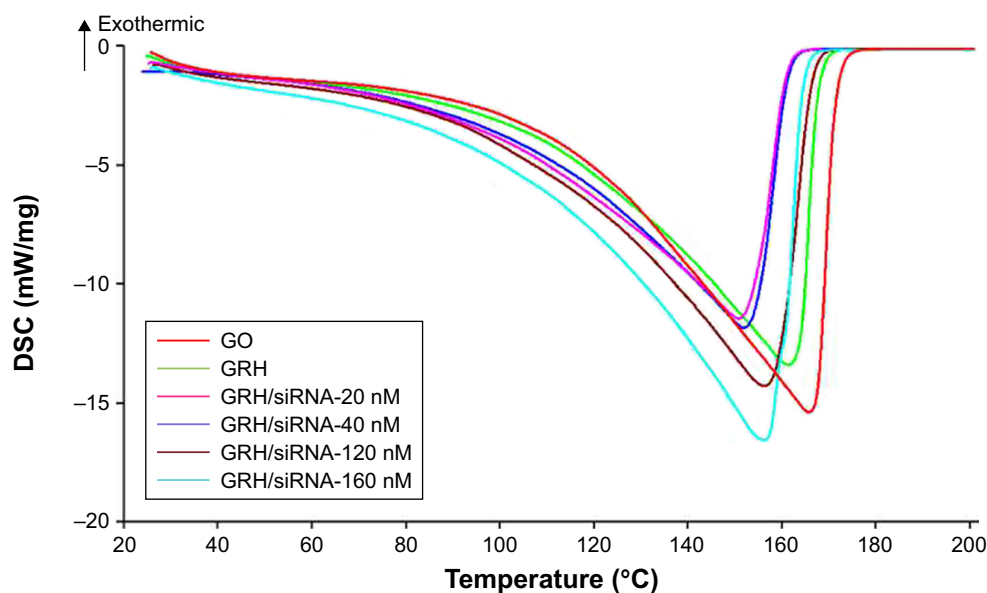


Figure 7 DSC thermograms of GO, GRH, and GRH/survivin-siRNA in 20 μ L diethyl pyrocarbonate.

Abbreviations: DSC, differential scanning calorimeter; GO, graphene oxide; GRH, GO-R8/anti-HER2; R8, octaarginine.

Cellular uptake of GRH/survivin-siRNA

The internalization of siRNA delivery was measured using a laser scanning confocal microscope. MCF-7 cells were transfected for 6 hours and treated with PBS medium solution (blank control), naked FAM-survivin-siRNA, and GRH/FAM-survivin-siRNA, Lipo 2000/FAM-survivin-siRNA (positive control). Figure 8 shows that green fluorescence (FAM-survivin-siRNA) was observed around the nucleus of MCF-7 cells in GRH/FAM-survivin-siRNA and Lipo 2000/FAM-survivin-siRNA compared with the naked FAM-survivin-siRNA group. It suggested that NS-siRNA was difficult to be transferred into the cytoplasm of MCF-7 cells. However, GRH/survivin-siRNA showed the high transfection efficiency. Therefore, GRH could effectively deliver siRNA into cells, which ensured the transfection ability, good cytoplasm accumulation, and desirable gene silencing efficacy of GRH/survivin-siRNA.

Cell proliferation inhibitory activity

The most important standard for the stabilized carrier is to measure the pharmacological activity of drug.^{38,39} In this study, tumor growth inhibitory activity of different concentrations of GRH/survivin-siRNA was measured by MTT assay against MCF-7 cells. MCF-7 cells were treated with GRH, survivin-siRNA, GRH/NC, GRH/survivin-siRNA, Lipo 2000/NC, and Lipo 2000/survivin-siRNA at the concentration of 30 nM, 60 nM, 90 nM, 120 nM, and 150 nM,

respectively. The results are shown in Figure 9. GRH, survivin-siRNA, GRH/NC, and Lipo 2000/NC were used as NC and Lipo 2000/survivin-siRNA served as a positive control. There was no significant difference between the cell viability of GRH, GRH/NC, NS-siRNA, and Lipo 2000/NC groups ($P > 0.05$), which suggested that they have no inhibitory activity. The GRH/survivin-siRNA group had lower significant difference than the groups of GRH/NC, GRH, survivin-siRNA, and Lipo 2000/NC ($P < 0.05$). The results indicated that survivin-siRNA was successfully delivered into MCF-7 cells by GRH and could effectively inhibit cell proliferation. Moreover, with the increase in the amount of GRH/survivin-siRNA, the cell viability was decreased from 58.6% to 51% significantly, which indicated that the cell proliferation inhibitory effect of GRH/survivin-siRNA showed a concentration-dependent manner.

Real-time PCR

The gene silencing efficiency of GRH/survivin-siRNA on mRNA level was evaluated by real-time PCR. GRH/NC was used as a NC and Lipo 2000/survivin-siRNA served as a positive control. The results are shown in Figure 10. The expression of survivin mRNA in the GRH/survivin-siRNA group was significantly reduced compared with the NC group and higher than the positive control group (0.5416 ± 0.0130) significantly ($P < 0.01$). The results indicated that GRH/survivin-siRNA could effectively downregulate the expression of survivin mRNA.

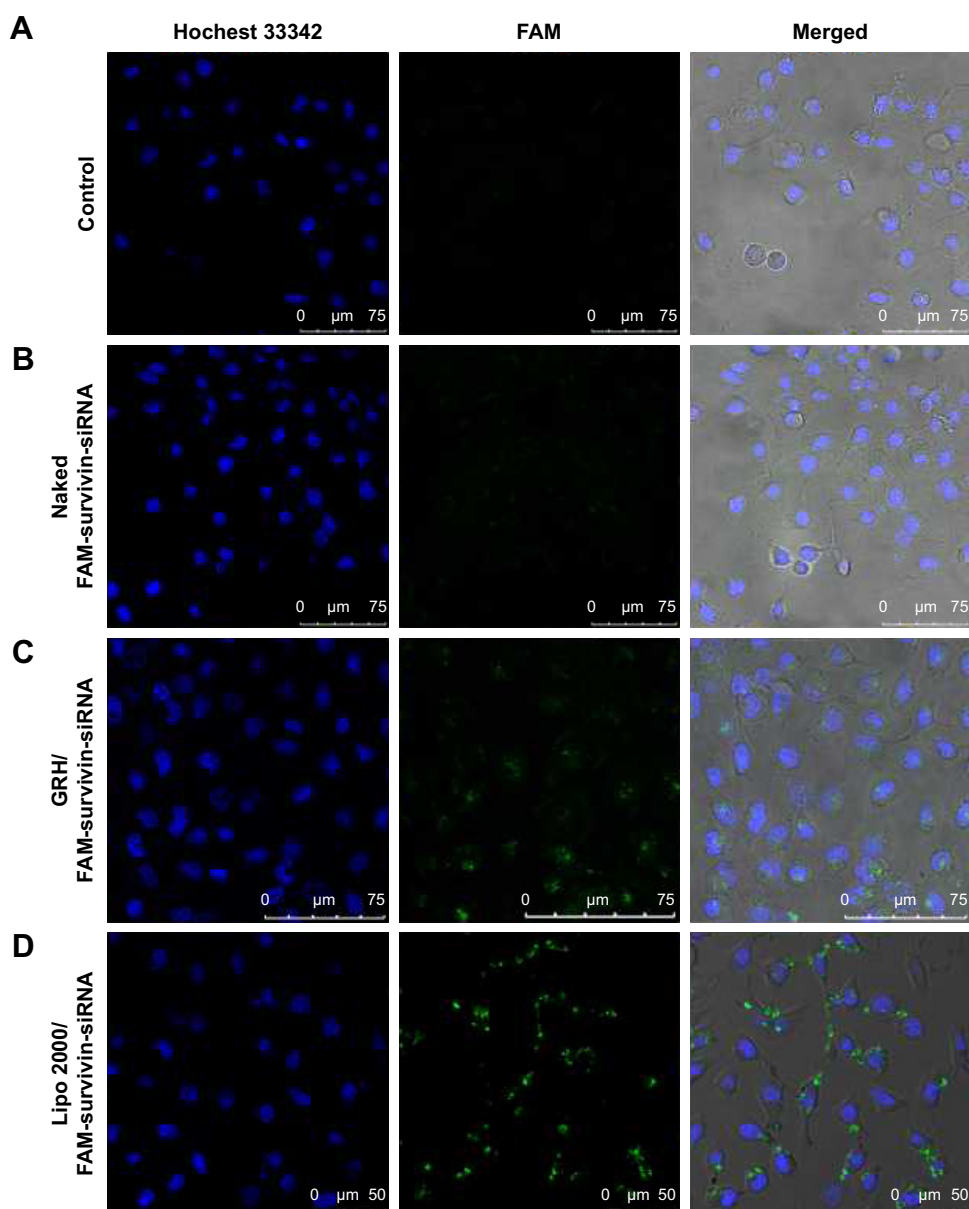


Figure 8 Confocal images of blank control (A), cells treated with naked FAM-survivin-siRNA (B), GRH/FAM-survivin-siRNA (C) and Lipo™ 2000/FAM-survivin-siRNA (D). **Abbreviations:** siRNA, small interfering RNA; GRH, GO-R8/anti-HER2; GO, graphene oxide; R8, octaarginine; FAM, carboxyfluorescein.

ELISA

ELISA is a recommended and preferred technique to measure the protein expression of GRH/survivin-siRNA as shown in Figure 11. The results of ELISA demonstrated that GRH/survivin-siRNA led to $50.86\% \pm 2.94\%$ inhibition of the expression of survivin protein in MCF-7 cells compared with the control. However, GRH/NC, NS-siRNA, and Lipo 2000/NC group exhibited no significant gene silencing effect ($P > 0.05$). These results reconfirmed that GRH/survivin-siRNA could obviously downregulate the survivin expression in desired protein level.

Antitumor of GRH/survivin-siRNA in vivo

The antitumor effect in vivo is an important standard for evaluating the efficiency of nonviral vector.^{30,40} The favorable antiproliferation effect of GRH/survivin-siRNA on MCF-7 cells offered us a confidence in its application in vivo for anti-tumor therapy as shown in Figure 12. The results indicated that the tumor volume (cm^3) of mice in naked siRNA (purple) and NS control (green) groups both grew very quickly within 10 days, and there was no significant difference between these 2 groups ($P > 0.05$), which suggested that the naked siRNA

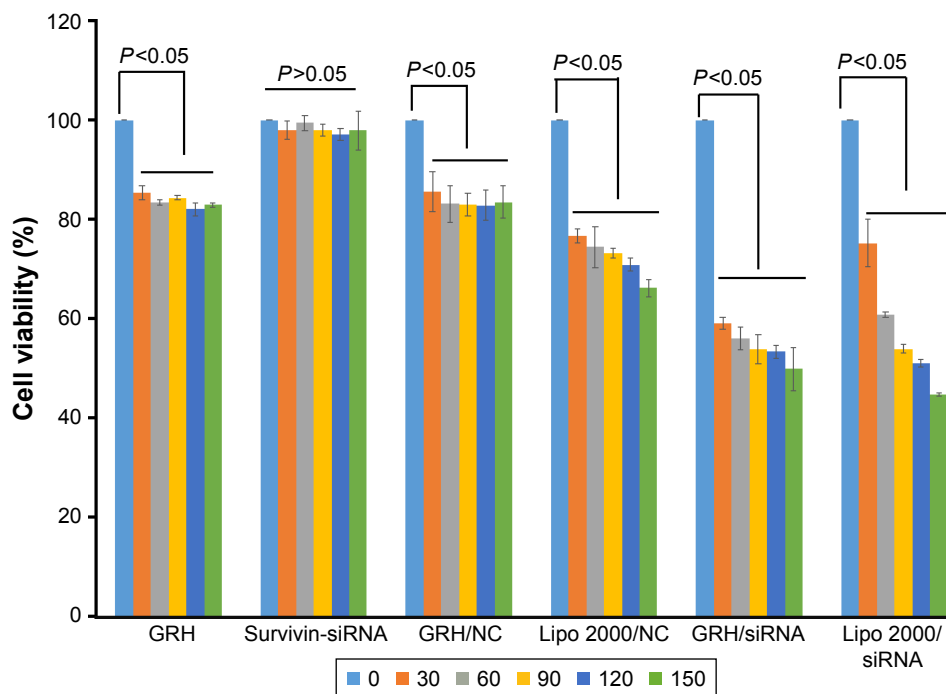


Figure 9 Anti-proliferation effect of GRH/survivin-siRNA at different concentrations on MCF-7 cells (n=3).
Abbreviations: GRH, GO-R8/anti-HER2; GO, graphene oxide; R8, octaarginine; NC, negative control.

could not inhibit the tumor growth. However, in the GRH/survivin-siRNA group (blue), the tumor grew very slowly and had no significant difference with positive control (red), which indicated that GRH/survivin-siRNA showed inhibitory effect on MCF-7 tumor growth in vivo.

Figure 13 shows that there was no significant difference between the carrier complex and the blank control, indicating that the carrier was safe and low toxic.

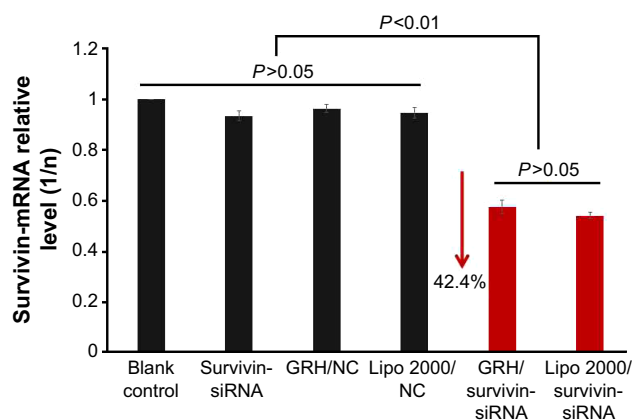


Figure 10 Survivin mRNA expression of GRH/survivin-siRNA-treated MCF-7 cells.
Note: Data are presented as average \pm SD, n=3.
Abbreviations: mRNA, messenger RNA; GO, graphene oxide; R8, octaarginine; GRH, GO-R8/anti-HER2; NC, negative control.

Figure 14 shows that there was no remarkable difference in tumor weight between NS-siRNA and NS control groups. But the tumor weight in the GRH/survivin-siRNA group was very significantly lower than those of NS-siRNA and blank control groups ($P < 0.01$). In addition, the differences in tumor size among these 4 groups could be obviously observed at Figure 14A. The tumor inhibitory rate of the GRH/survivin-siRNA group (59.19%) was much higher than that of the NS-siRNA group (4.52%), and less lower than the positive control groups (62.17%, $P > 0.05$). These results were consistent with the results of tumor volume. Therefore, it was concluded that GRH vector was able to deliver the survivin-siRNA and effectively inhibit the tumor growth in vivo.

Targeting efficiency of GRH/survivin-siRNA in vivo was estimated by controlled experiment. Figure 15 shows that there was significant difference in tumor weight between GO-R8 (GR)/survivin-siRNA and GRH/survivin-siRNA, and the tumor weight in the GRH/survivin-siRNA group was very significantly lower than GR/survivin-siRNA ($P < 0.01$). It was inferred that GRH/survivin-siRNA had good targeting efficiency and tumor inhibitory effect.

Cytotoxicity

Excellent gene carrier has not only high transfection efficiency but also low toxicity.^{41,42} Cytotoxicity of GRH was evaluated

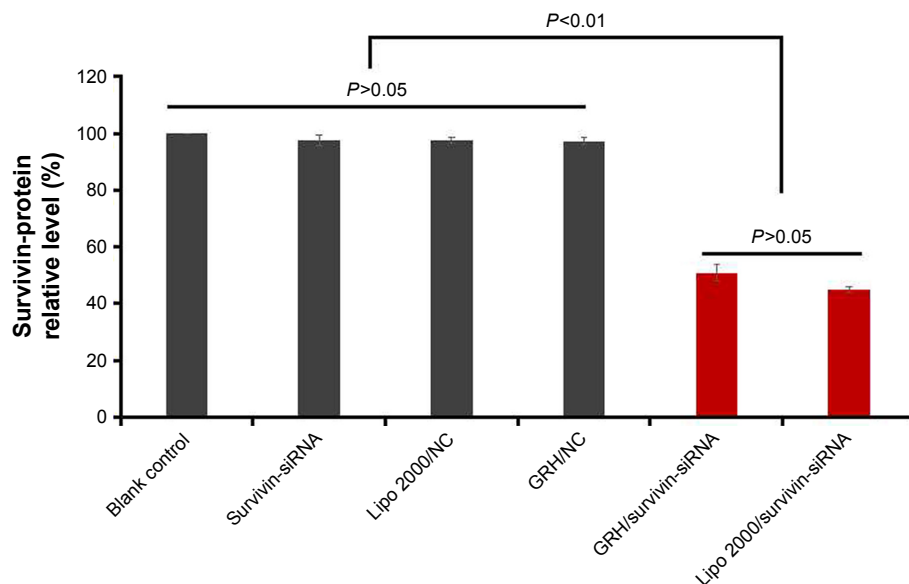


Figure 11 Protein expression of GRH/survivin-siRNA-treated MCF-7 cells.

Note: Data are presented as average \pm SD, $n=3$.

Abbreviations: GRH, GO-R8/anti-HER2; GO, graphene oxide; R8, octaarginine; NC, negative control.

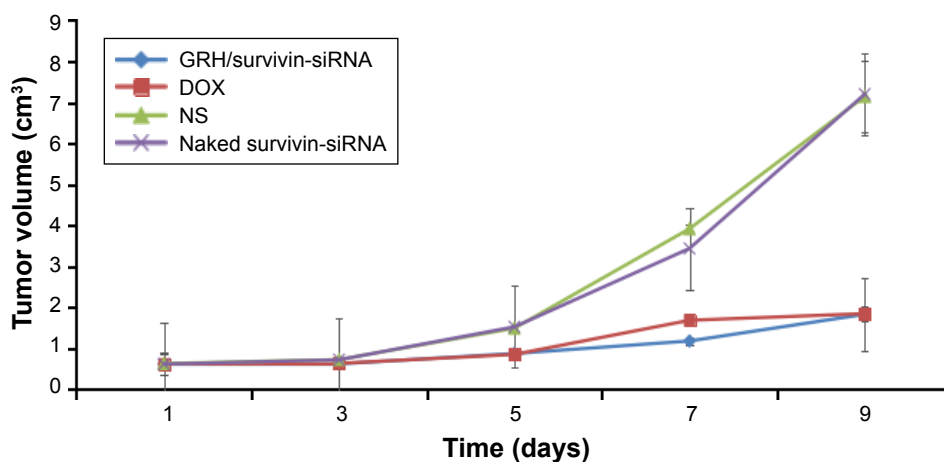


Figure 12 Tumor volume (cm^3) of the group of control NS-siRNA, GRH/survivin-siRNA, and DOX.

Notes: NS was used as blank control. Naked siRNA was used as negative control ($n=10$).

Abbreviations: NS, naked survivin; GRH, GO-R8/anti-HER2; GO, graphene oxide; R8, octaarginine; DOX, doxorubicin.

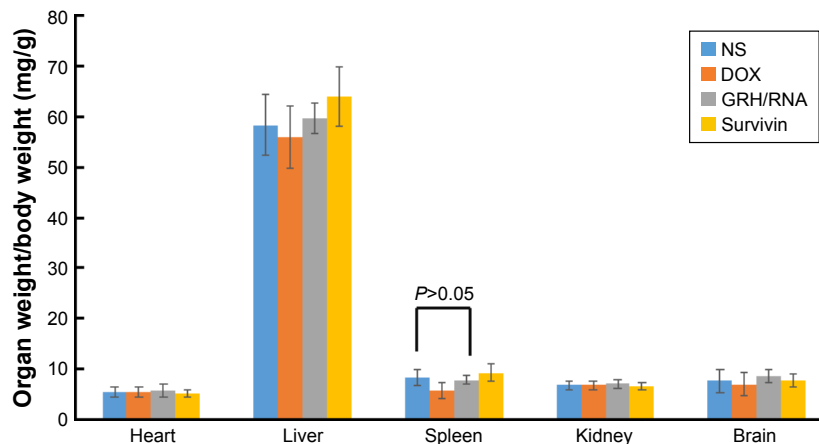


Figure 13 The organ weight/body weight.

Abbreviations: NS, naked survivin; GRH, GO-R8/anti-HER2; GO, graphene oxide; R8, octaarginine.

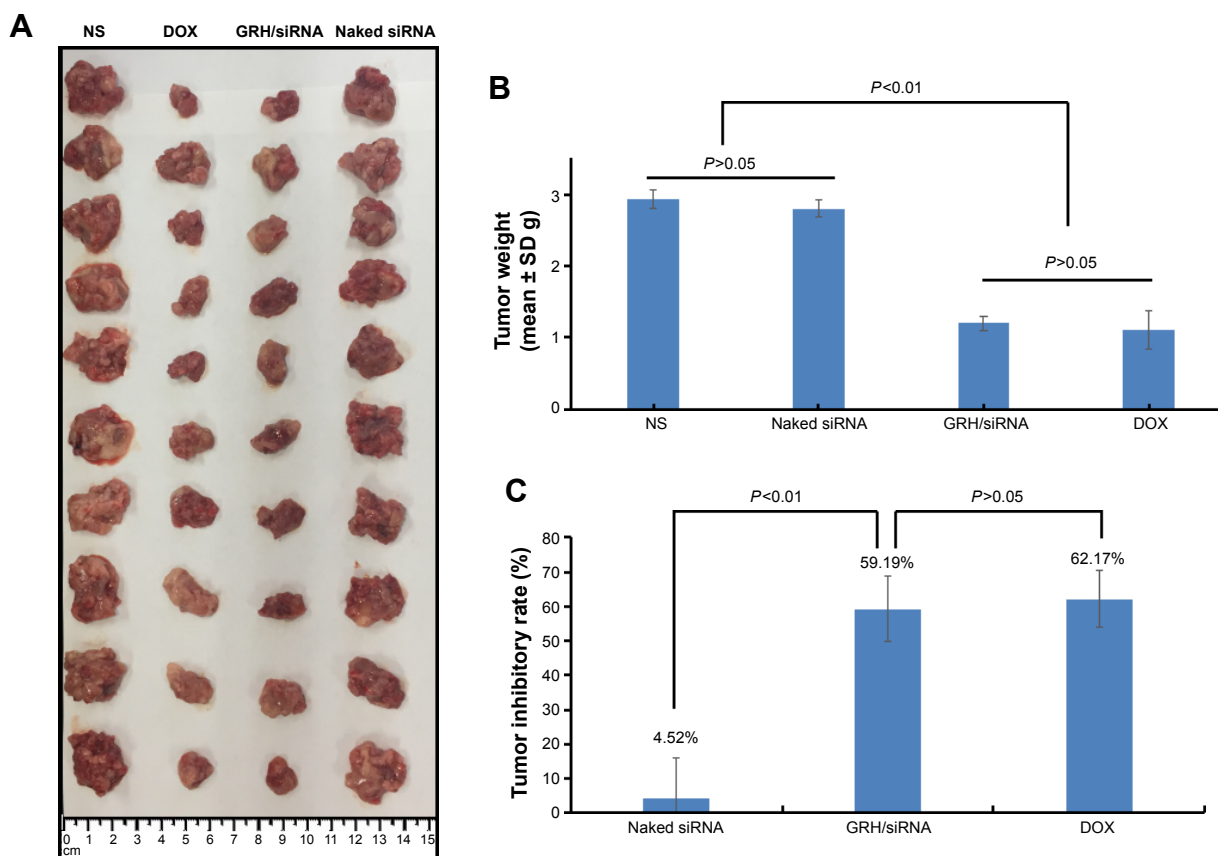


Figure 14 The antitumor effect of NS, DOX, GRH/survivin-siRNA, and NS-siRNA in vivo.

Note: Image of tumors (A), tumor weight (B), and tumor inhibitory rate (C) (n=10).

Abbreviations: NS, naked survivin; GRH, GO-R8/anti-HER2; GO, graphene oxide; R8, octaarginine; DOX, doxorubicin.

using MTT assay on MCF-7 cell lines (Figure 16). The concentrations of GRH ranged from 5 $\mu\text{g}/\text{mL}$ to 120 $\mu\text{g}/\text{mL}$. The results showed that all concentrations of GRH did not display the testable cytotoxicity.

Conclusion

A development approach toward tumor therapy mediated by GRH had been established as a safe and effective vector for siRNA delivery. The results demonstrated that

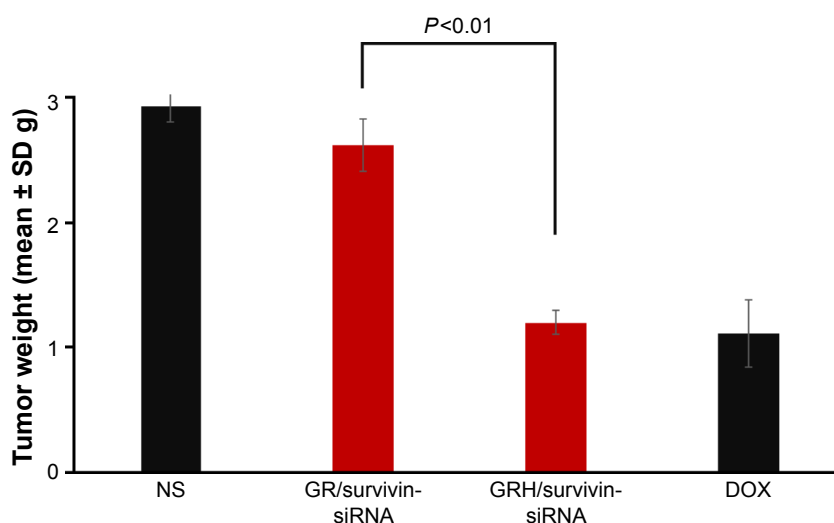


Figure 15 Targeting efficiency of NS, GR/survivin-siRNA, GRH/survivin-siRNA, and DOX in vivo.

Abbreviations: NS, naked survivin; GR, GO-R8; GRH, GO-R8/anti-HER2; GO, graphene oxide; R8, octaarginine; DOX, doxorubicin.

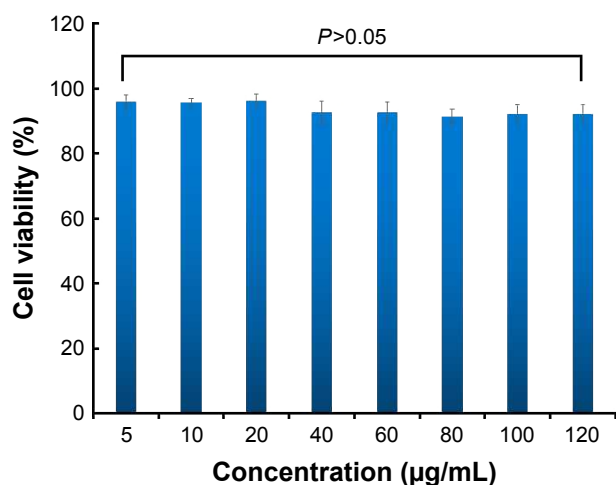


Figure 16 Cytotoxicity assay using MTT method.
Note: Data are presented as average \pm SD, n=3.

survivin-siRNA not only loaded onto the surface of GRH and successfully delivered into MCF-7 cells but also induced effective gene-silencing effects. Meanwhile, it showed a strong inhibitory effect on tumor growth in vivo and in vitro. It had no testable cytotoxicity. The final experimental results showed that GRH was an efficient and low toxic gene delivery carrier.

Acknowledgments

This work was supported by National Natural Science Foundation (81502688), Beijing Natural Science Foundation Program and Scientific Research Key Program of Beijing Municipal Commission of Education (KM201810025019), the Basic-Clinical Key Research Grant (16JL72, 17JL67) from Capital Medical University, the Importation and Development of High-Caliber Talents Project of Beijing Municipal Institutions (2013–2015), and China's 55 of postdoctoral scientific research funds (2014M550768). The authors gratefully acknowledge the supports from Beijing area Major Laboratory of Peptide and Small Molecular Drugs, Engineering Research Center of Endogenous Prophylactic of Ministry of Education of China, and Beijing Laboratory of Biomedical Materials.

Disclosure

The authors report no conflicts of interest in this work.

References

1. Orlacchio A, Bernardi G, Oracchio A, Martino S. RNA interference as a tool for Alzheimer's disease therapy. *Mini Rev Med Chem*. 2007;7(11):1166–1176.
2. Pai SI, Lin YY, Macaes B, Meneshian A, Hung CF, Wu TC. Prospects of RNA interference therapy for cancer. *Gene Ther*. 2006;13(6):464–477.

3. Ballarín-González B, Howard KA. Polycation-based nanoparticle delivery of RNAi therapeutics: adverse effects and solutions. *Adv Drug Deliv Rev*. 2012;64(15):1717–1729.
4. Hartono SB, Phuoc NT, Yu M, et al. Functionalized large pore mesoporous silica nanoparticles for gene delivery featuring controlled release and co-delivery. *J Mater Chem B*. 2014;2(6):718–726.
5. Dreyer DR, Park S, Bielawski CW, Ruoff RS. The chemistry of graphene oxide. *Chem Soc Rev*. 2009;39(1):228–240.
6. Bao H, Pan Y, Ping Y, et al. Chitosan-functionalized graphene oxide as a nanocarrier for drug and gene delivery. *Small*. 2011;7(11):1569–1578.
7. Wen H, Dong C, Dong H, et al. Engineered redox-responsive PEG detachment mechanism in PEGylated nano-graphene oxide for intracellular drug delivery. *Small*. 2012;8(5):760–769.
8. Liu G, Shen H, Mao J, et al. Transferrin modified graphene oxide for glioma-targeted drug delivery: in vitro and in vivo evaluations. *ACS Appl Mater Interfaces*. 2013;5(15):6909.
9. Kavitha T, Abdi SIH, Park SY. pH-sensitive nanocargo based on smart polymer functionalized graphene oxide for site-specific drug delivery. *Phys Chem Chem Phys*. 2013;15(14):5176–5185.
10. Xu H, Fan M, Elhissi AM, et al. PEGylated graphene oxide for tumor-targeted delivery of paclitaxel. *Nanomedicine*. 2015;10(8):1247–1262.
11. Cheng Z, Feng J, Lin X, et al. Continuous release of bone morphogenetic protein-2 through nano-graphene oxide-based delivery influences the activation of the NF- κ B signal transduction pathway. *Int J Nanomedicine*. 2017;12:1215–1226.
12. Feng L, Zhang S, Liu Z. Graphene based gene transfection. *Nanoscale*. 2011;3(3):1252–1257.
13. Kim H, Namgung R, Singha K, Oh IK, Kim WJ. Graphene oxide-polyethylenimine nanoconstruct as a gene delivery vector and bioimaging tool. *Bioconjug Chem*. 2011;22(12):2558.
14. Chen B, Liu M, Zhang L, et al. Polyethylenimine-functionalized graphene oxide as an efficient gene delivery vector. *J Mater Chem*. 2011;21(21):7736–7741.
15. Dong H, Ding L, Yan F, Ji H, Ju H. The use of polyethylenimine-grafted graphene nanoribbon for cellular delivery of locked nucleic acid modified molecular beacon for recognition of microRNA. *Biomaterials*. 2011;32(15):3875–3882.
16. Wang C, Wang X, Lu T, et al. Multi-functionalized graphene oxide complex as a plasmid delivery system for targeting hepatocellular carcinoma therapy. *RSC Adv*. 2016;6(27):22461–22468.
17. Feng L, Yang X, Shi X, et al. Polyethylene glycol and polyethylenimine dual-functionalized nano-graphene oxide for photothermally enhanced gene delivery. *Small*. 2013;9(11):1989–1997.
18. Yang X, Niu G, Cao X, et al. The preparation of functionalized graphene oxide for targeted intracellular delivery of siRNA. *J Mater Chem*. 2012;22(14):6649–6654.
19. Imani R, Emami SH, Faghihi S. Synthesis and characterization of an octarginine functionalized graphene oxide nano-carrier for gene delivery applications. *Phys Chem Chem Phys*. 2015;17(9):6328–6339.
20. Rajendran L, Knolker HJ, Simons K. Subcellular targeting strategies for colloidal biomaterial on cellular uptake and cell functions. *Biomaterials*. 2013;1:896–911.
21. Smolewski P, Robak T. Inhibitors of apoptosis proteins (IAPs) as potential molecular targets for therapy of hematological malignancies. *Curr Mol Med*. 2011;11(8):633–649.
22. Mobahat M, Narendran A, Riabowol K. Survivin as a preferential target for cancer therapy. *Int J Mol Sci*. 2014;15(2):2494–2516.
23. Zhou R, Zhang LZ, Wang RZ. Effect of celecoxib on proliferation, apoptosis, and survivin expression in human glioma cell line U251. *Chin J Cancer*. 2010;29(3):294–299.
24. Hussain SF, Kong LY, Jordan J, et al. A novel small molecule inhibitor of signal transducers and activators of transcription 3 reverses immune tolerance in malignant glioma patients. *Cancer Res*. 2007;67(20):9630–9636.
25. Na M, Su YT, Zhou N, et al. Carboxylated graphene oxide functionalized with β -cyclodextrin – engineering of a novel nanohybrid drug carrier. *Int J Biol Macromol*. 2016;93(Pt A):117–122.

26. Goenka S, Sant V, Sant S. Graphene-based nanomaterials for drug delivery and tissue engineering. *J Control Release*. 2014;173(1):75–88.
27. Hu W, Peng C, Lv M, et al. Protein corona-mediated mitigation of cytotoxicity of graphene oxide. *ACS Nano*. 2011;5(5):3693–3700.
28. Ren L, Zhang Y, Cui C, et al. Functionalized graphene oxide for anti-VEGF siRNA delivery: preparation, characterization and evaluation in vitro and in vivo. *RSC Adv*. 2017;7(33):20553–20566.
29. Elbakry A, Zaky A, Liebl R, Rachel R, Goepferich A, Breunig M. Layer-by-layer assembled gold nanoparticles for siRNA delivery. *Nano Lett*. 2009;9(5):2059–2064.
30. Xie Y, Qiao H, Su Z, Chen M, Ping Q, Sun M. PEGylated carboxymethyl chitosan/calcium phosphate hybrid anionic nanoparticles mediated hTERT siRNA delivery for anticancer therapy. *Biomaterials*. 2014;35(27):7978–7991.
31. Choi JH, Jang JY, Joung YK, Kwon MH, Park KD. Intracellular delivery and anti-cancer effect of self-assembled heparin-Pluronic nanogels with RNase A. *J Control Release*. 2010;147(3):420–427.
32. Cui C, Wang Y, Zhao W, et al. RGDS covalently surfaced nanodiamond as a tumor targeting carrier of VEGF-siRNA: synthesis, characterization and bioassay. *J Mater Chem B*. 2015;3(48):9260–9268.
33. Xu A, Zhou L, Deng Y, et al. A carboxymethyl chitosan and peptide-decorated polyetheretherketone ternary biocomposite with enhanced antibacterial activity and osseointegration as orthopedic/dental implants. *J Mater Chem B*. 2016;4(10):1878–1890.
34. Chen C, Ridzon DA, Broomer AJ, et al. Real-time quantification of microRNAs by stem-loop RT-PCR. *Nucleic Acids Res*. 2005;33(20):179.
35. Thomas E. Laser pointer and the tyndall effect. *J Chem Educ*. 1996;73(73):470.
36. Ficarra R, Ficarra P, Di BM, et al. Study of beta-blockers/beta-cyclodextrins inclusion complex by NMR, DSC, X-ray and SEM investigation. *J Pharm Biomed Anal*. 2000;23(1):33–40.
37. Temming K, Schiffelers RM, Molema G, Kok RJ. RGD-based strategies for selective delivery of therapeutics and imaging agents to the tumour vasculature. *Drug Resist Updat*. 2005;8(6):381–402.
38. Maver U, Godec A, Bele M, et al. Novel hybrid silica xerogels for stabilization and controlled release of drug. *Int J Pharm*. 2007;330(1–2):164–174.
39. Wang W, Fang C, Wang X, et al. Modifying mesoporous silica nanoparticles to avoid the metabolic deactivation of 6-mercaptopurine and methotrexate in combinatorial chemotherapy. *Nanoscale*. 2013;5(14):6249–6253.
40. Beloor J, Choi CS, Nam HY, et al. Arginine-grafted biodegradable polymer for the systemic delivery of therapeutic siRNA. *Biomaterials*. 2012;33(5):1640–1650.
41. Kaur R, Badea I. Nanodiamonds as novel nanomaterials for biomedical applications: drug delivery and imaging systems. *Int J Nanomedicine*. 2013;8:203.
42. Schrand AM, Huang H, Carlson C, et al. Are diamond nanoparticles cytotoxic? *J Phys Chem B*. 2007;111(1):2–7.

Drug Design, Development and Therapy

Publish your work in this journal

Drug Design, Development and Therapy is an international, peer-reviewed open-access journal that spans the spectrum of drug design and development through to clinical applications. Clinical outcomes, patient safety, and programs for the development and effective, safe, and sustained use of medicines are the features of the journal, which

Submit your manuscript here: <http://www.dovepress.com/drug-design-development-and-therapy-journal>

Dovepress

has also been accepted for indexing on PubMed Central. The manuscript management system is completely online and includes a very quick and fair peer-review system, which is all easy to use. Visit <http://www.dovepress.com/testimonials.php> to read real quotes from published authors.